

## Electronic Supplementary Information

# Nanostructured SnS with Inherent Anisotropic Optical Properties for High Photoactivity<sup>†</sup>

*Malkeshkumar Patel,<sup>\*ab‡</sup> Arvind Chavda,<sup>a</sup> Indrajit Mukhopadhyay,<sup>a</sup> Joondong Kim,<sup>b</sup> and Abhijit Ray<sup>\*a</sup>*

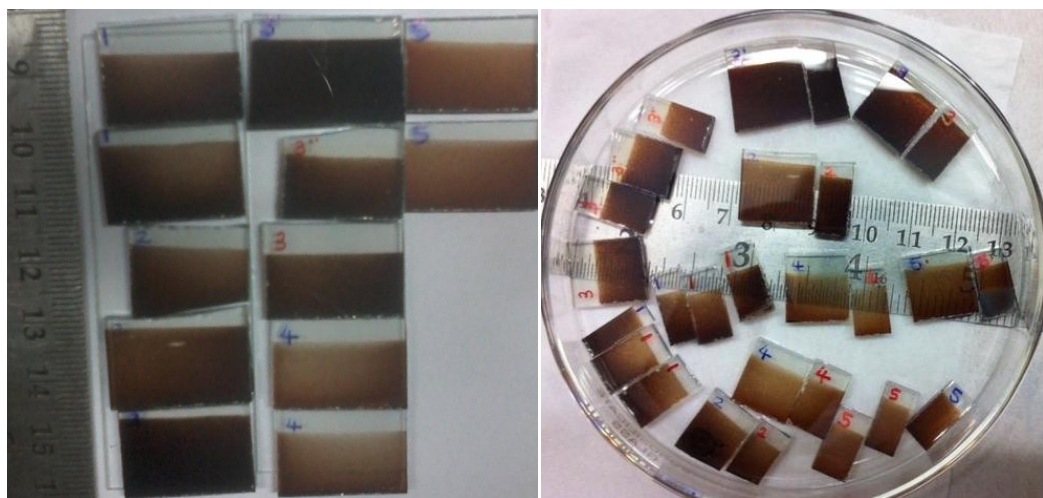
<sup>a</sup> Solar Research and Development Center, Pandit Deendayal Petroleum University, Gandhinagar 382007, Gujarat, India. Fax: 91 79 23275030; Tel: 91 79 23275304; E-mail: [mpethani@gmail.com](mailto:mpethani@gmail.com); [abhijit.ray1974@gmail.com](mailto:abhijit.ray1974@gmail.com)

<sup>b</sup> Photoelectric and Energy Device Application Lab (PEDAL), Department of Electrical Engineering, Incheon National University, 119 Academy Rd. Yeonsu Incheon, 406772, Korea.

<sup>†</sup> Electronic Supplementary Information (ESI) available: [details of any supplementary information available should be included here]. See DOI: 10.1039/b000000x/

<sup>‡</sup> Present address.

**Section S1. The deposited SnS thin films on the F:SnO<sub>2</sub> coated glass substrate**



## Section S2. Structural model of the layered tin monosulfide (SnS)

### S2.1. Structural properties of nanostructured SnS thin films

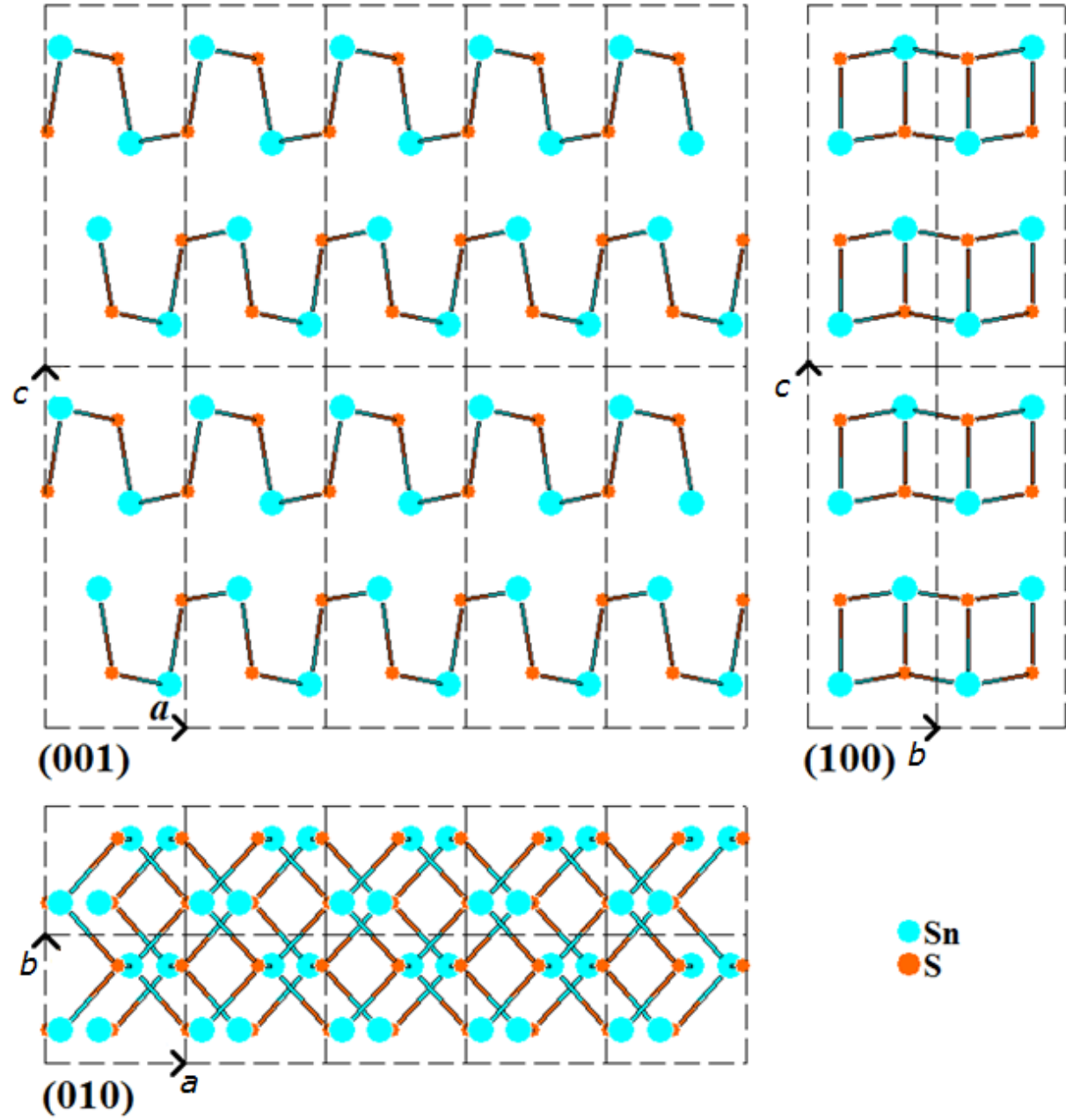


**Figure S1.** Structural presentation of super cell of  $\alpha$ -SnS ( $Pbnm$  (62)) in various lattice directions, where  $a$ ,  $b$  and  $c$  are the lattice parameters. Aqua and orange spheres represent Sn and S atoms, respectively.

**Table S1.** Table of reflection parameters derived from the X-ray power patterns for wavelength of 1540.6 nm with considering the Lorentz & Polarization factors with Pseudo-voigt profile function with  $2\theta$  step =  $0.02^\circ$  with FWHM =  $0.5^\circ$ , for SnS unit cell with COD-Code 9008785.

$2\theta$ (degree)	$d$ - spacing (Å)	Intensity	$h$	$k$	$l$	$2\theta$ (degree)	$d$ - spacing (Å)	Intensity	$h$	$k$	$l$
22.00	4.04	4.83E+05	1	0	1	66.44	1.41	1.22E+05	1	2	5
26.01	3.42	8.56E+05	1	0	2	66.64	1.40	1.04E+05	1	1	7
27.49	3.24	1.00E+06	0	1	2	66.90	1.40	7.80E+04	3	0	2
30.48	2.93	7.26E+05	1	1	0	66.90	1.40	7.71E+04	0	0	8
31.54	2.83	1.45E+06	1	1	1	68.80	1.36	1.79E+05	2	2	3
31.65	2.82	4.85E+04	1	0	3	69.18	1.36	1.17E+05	3	1	0
32.00	2.80	9.56E+05	0	0	4	69.83	1.35	4.21E+04	3	0	3
38.30	2.35	1.51E+04	1	0	4	71.49	1.32	4.27E+04	0	1	8
39.07	2.30	6.93E+05	1	1	3	72.83	1.30	2.46E+04	2	2	4
39.36	2.29	8.24E+04	0	1	4	72.83	1.30	8.79E+04	1	2	6
41.69	2.17	4.60E+04	2	0	0	73.28	1.29	6.34E+04	0	3	2
42.50	2.13	3.14E+05	2	0	1	73.65	1.29	8.25E+04	2	0	7
44.78	2.02	4.71E+05	1	1	4	74.34	1.28	3.02E+04	3	1	3
45.55	1.99	3.86E+05	0	2	0	74.79	1.27	5.20E+04	1	3	0
45.63	1.99	1.93E+05	1	0	5	75.28	1.26	8.39E+04	1	1	8
48.52	1.87	3.80E+05	2	1	1	75.35	1.26	1.07E+05	1	3	1
48.60	1.87	2.61E+05	2	0	3	77.89	1.23	6.96E+04	2	2	5
51.13	1.79	1.10E+05	1	2	1	78.07	1.22	2.86E+04	2	1	7
51.36	1.78	2.93E+05	1	1	5	78.26	1.22	1.53E+05	3	1	4
53.20	1.72	2.36E+05	1	2	2	78.87	1.21	2.09E+04	3	0	5
53.49	1.71	3.15E+04	2	0	4	79.81	1.20	8.21E+04	1	3	3
53.49	1.71	1.13E+05	1	0	6	80.35	1.19	6.34E+04	1	0	9
54.09	1.69	1.65E+05	2	1	3	83.04	1.16	5.05E+04	3	2	1
54.32	1.69	1.87E+05	0	1	6	83.65	1.16	7.42E+04	1	3	4
56.52	1.63	2.24E+04	1	2	3	84.68	1.14	3.85E+04	1	1	9
56.74	1.62	3.53E+05	0	2	4	84.68	1.14	8.14E+04	3	2	2
58.67	1.57	1.27E+04	2	1	4	84.68	1.14	8.12E+04	0	2	8
59.37	1.56	7.79E+04	2	0	5	84.92	1.14	4.19E+04	3	0	6
63.44	1.47	2.45E+04	2	2	0	86.32	1.13	1.22E+04	2	1	8
64.05	1.45	1.80E+05	2	2	1	86.38	1.13	7.09E+04	2	3	1
64.24	1.45	2.36E+05	2	1	5	87.41	1.11	4.78E+04	3	2	3
65.11	1.43	4.95E+04	3	0	1	88.56	1.10	6.28E+04	1	3	5

## S2.2. Phase data of $\alpha$ -SnS material

Crystal system	Orthorhombic
Space-group	$P b n m$ (62)
Cell parameters	$a = 4.33 \text{ \AA}$ , $b = 3.98 \text{ \AA}$ , $c = 11.18 \text{ \AA}$
Cell ratio	$a/b = 1.0879$ , $b/c = 0.3559$ , $c/a = 2.5819$
Cell volume	$192.67 \text{ \AA}^3$
Pearson code	oP0

The lattice parameters of the spray deposited nanostructured SnS thin films are calculated by the following relation,

$$\frac{1}{d^2} = \left( \frac{h^2}{a^2} + \frac{k^2}{b^2} + \frac{l^2}{c^2} \right)$$

## Section S3. Substrate characterization

### S3.1. XRD of FTO coated glass substrate.

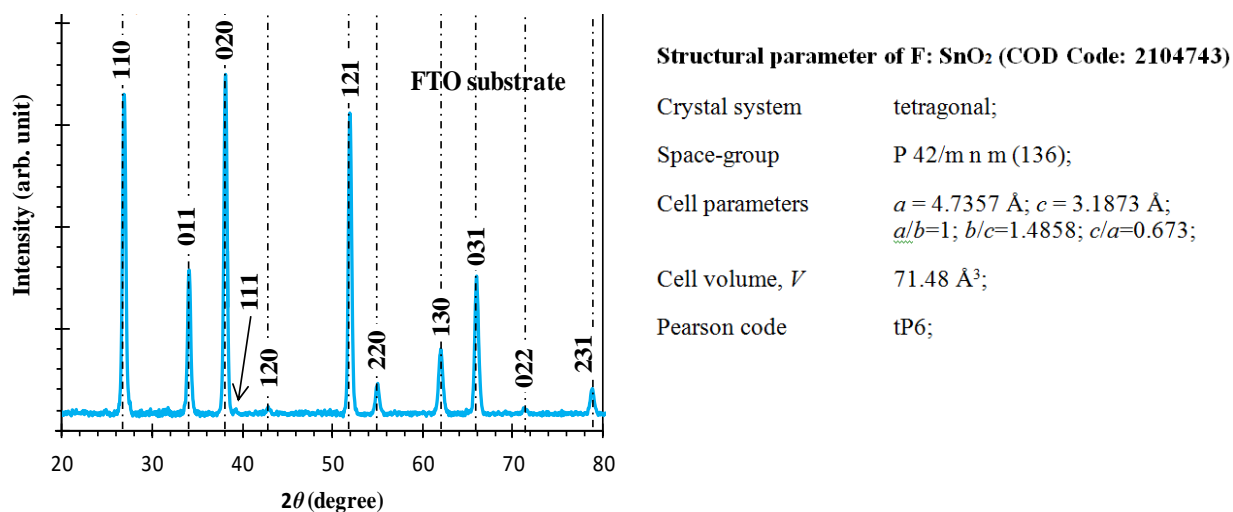


**Figure S2** XRD of F:SnO<sub>2</sub> (FTO) coated glass substrate.

### S3.2. Physical morphological properties of F:SnO<sub>2</sub> coated glass substrate

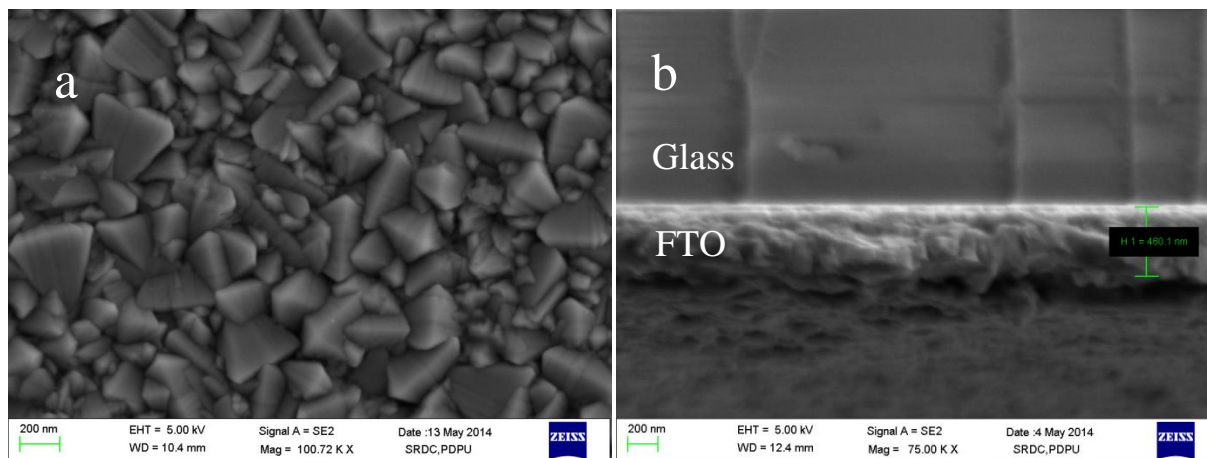


**Figure S3.** FESEM images of F:SnO<sub>2</sub> coated glass substrate (a) topography and (b) cross sectional. The thickness of FTO layer is ~500 nm were confirmed.

## Section S4. Surface morphology of FTO and SnS thin films

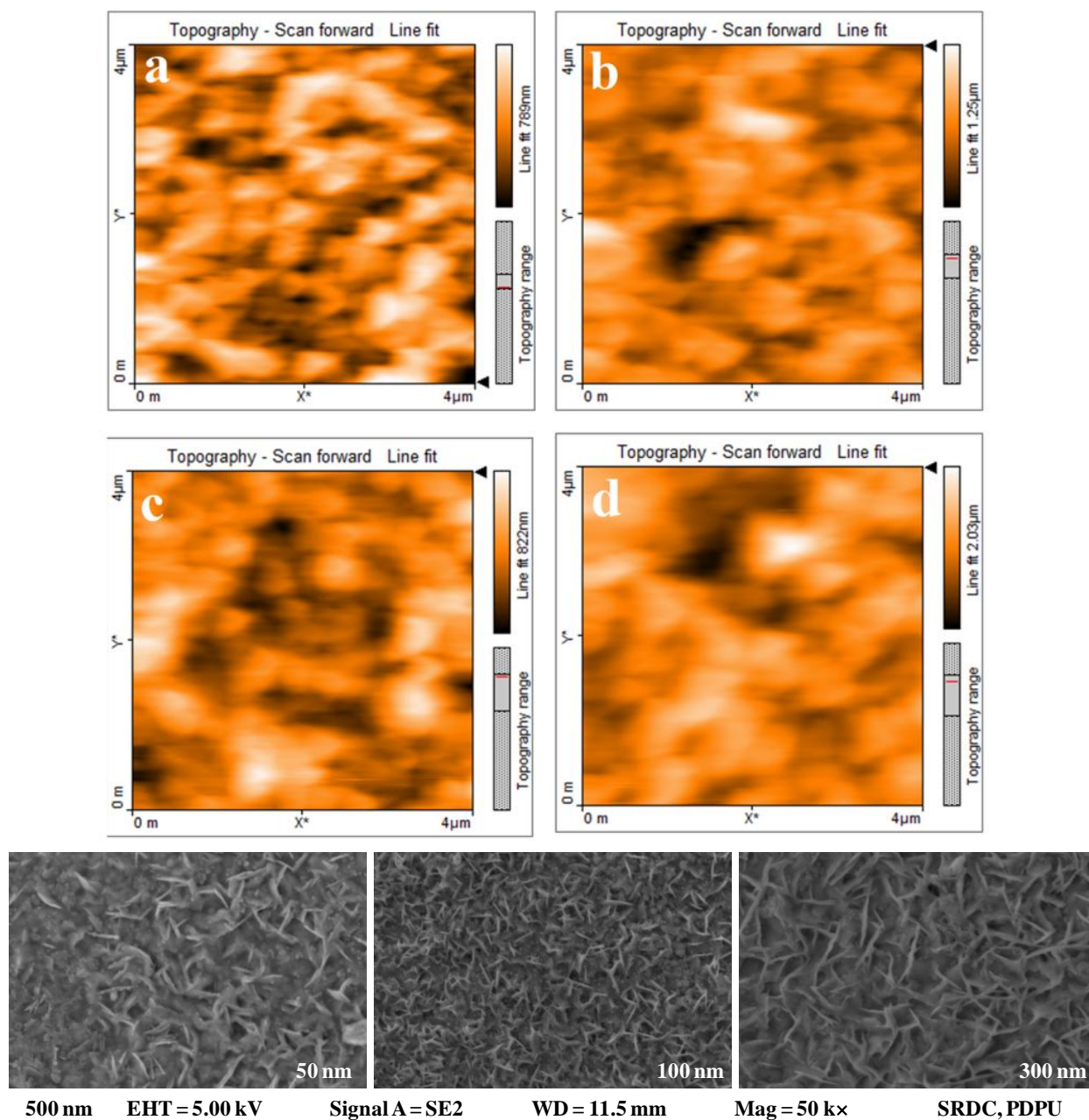


**Figure S4.** Atomic force micrograph of (a) FTO, (b) SnS thin films having thickness of 100 nm, (c) 250 nm, (d) 450 nm and (e) FESEM images of SnS thin films having various thicknesses from 50 nm to 300 nm.

**Table S2.** Surface morphology analysis performed from the AFM data of SnS thin films having different thickness of 100, 250 and 450 nm.

Image No.	Material	Scan Area ( $\mu\text{m}^2$ )	Planar Area, $A_P(\text{m}^2)$	Surface Area, $A_{surface}(\text{m}^2)$	$A_P/A_{surface}$
3342	FTO	$4 \times 4$	1.6E-11	2.724E-11	1.70
3343		$4 \times 4$	1.6E-11	2.737E-11	1.71
3344	SnS (100 nm)	$4 \times 4$	1.6E-11	2.548E-11	1.59
3345		$1 \times 1$	1E-12	1.840E-12	1.84
3346		$1 \times 1$	1E-12	2.031E-12	2.03
3337	SnS (250 nm)	$4 \times 4$	1.6E-11	2.197E-11	1.37
3338		$4 \times 4$	1.6E-11	2.334E-11	1.46
3339		$4 \times 4$	1.6E-11	2.163E-11	1.35
3340		$4 \times 4$	1.6E-11	2.299E-11	1.44
3341		$1 \times 1$	1E-12	1.747E-12	1.75
3347	SnS (450 nm)	$4 \times 4$	1.6E-11	3.068E-11	1.92
3348		$4 \times 4$	1.6E-11	3.317E-11	2.07
3349		$1 \times 1$	1E-12	2.305E-12	2.31
3350		$1 \times 1$	1E-12	2.474E-12	2.47
3351		$1 \times 1$	1E-12	2.427E-12	2.43



## Section S5. Electronic band gap calculation and potential distribution in the depletion layer of nanostructured SnS photoanode

**Table S3.** Summary of considered the physical constant and material properties of SnS thin film for calculation of donor carrier concentration and space charge width of photoanode.

Physical/material constant	Value	Unit	Remarks
Boltzmann constant, $k$	$1.38 \times 10^{-23}$	J / K	$8.62 \times 10^{-05}$ eV / K
Temperature, $T$	300	K	
Effective density of states for electrons in conduction band, $N_C$	$2.25 \times 10^{18}$	$\text{cm}^{-3}$	
Donor carrier concentration, $N_D$	$10^{15}$ to $5 \times 10^{17}$	$\text{cm}^{-3}$	
Effective mass of electron, $m_e$	$0.24 m_0$		[1]
Mass of electron in free space, $m_0$	$9.1094 \times 10^{-31}$	kg	
Planck's constant, $h$	$6.62607 \times 10^{-34}$	eV s	
Electron charge, $q$	$1.6021 \times 10^{-19}$	C	
Dielectric constant of SnS, $\epsilon_r$	$13 \epsilon_0$		[1]
Free space dielectric constant, $\epsilon_0$	$8.8542 \times 10^{-12}$	F / m	

The effective density of states for electrons in the conduction band  $N_C$  is determined using following relation,

$$N_C = 2 \left( \frac{2\pi m_e kT}{h^2} \right)^{\frac{3}{2}},$$

From the Mott-Schottky results, the position of the band edges for nanostructured SnS with respect to the vacuum level can be calculated by knowing the position of the valence band edge with respect to the vacuum level which is denoted here by  $E$ ,

$$E = E_{ref} + \Delta E_F + V_H + V_{FB},$$

where,  $E_{ref} = 4.644$  represents the absolute potential of Ag/AgCl below the vacuum level,

$\Delta E_F = E_F - E_V$  which is the difference between Fermi level ( $E_F$ ) and the valence band edge ( $E_V$ ) and

$V_H = 2.3kT/q$  (PZC -  $pH$ ) is Helmholtz potential between SnS electrode and electrolyte. Here PZC refers to the potential at zero charge at SnS/electrolyte surface.

$V_{FB}$  is the flat band potential, which is determined from the Mott-Schottky analysis. Since the flat-band potential was determined at the experimental value of PZC,  $V_H$  can be neglected [2].

$\Delta E_F$  is determined using the following relation,

$$\begin{aligned} E_C - E_F &= -kT \ln \left( \frac{N_D}{N_C} \right), \\ &= -8.62 \times 10^{-5} \text{ (eV/K)} \times 300 \text{ (K)} \times \ln (1 \times 10^{15} / 2.25 \times 10^{18}) \\ \Delta E_F &= 0.1995 \text{ eV} \end{aligned}$$

Hence,

$$E_V = 4.64 + 0.2 + 0.5 = 5.34 \text{ eV}$$

The following expression used for the space charge width,

$$W = \sqrt{\frac{2\epsilon_0\epsilon_r}{qN_A} \left( \phi_{sc} - \frac{kT}{q} \right)}$$

For the flat band condition the following relation are employed for capacitance-voltage characteristics,

$$\frac{1}{C^2} = \frac{2}{\epsilon_o\epsilon_r q N_D A^2} \left( \phi_{sc} - \frac{kT}{q} \right)$$

where,  $A$  and  $\phi_{sc}$  are active area and applied potential of the SnS/electrolyte interface, respectively [3].

## Section S6. Study of reproducibility of nanostructured SnS photoanode

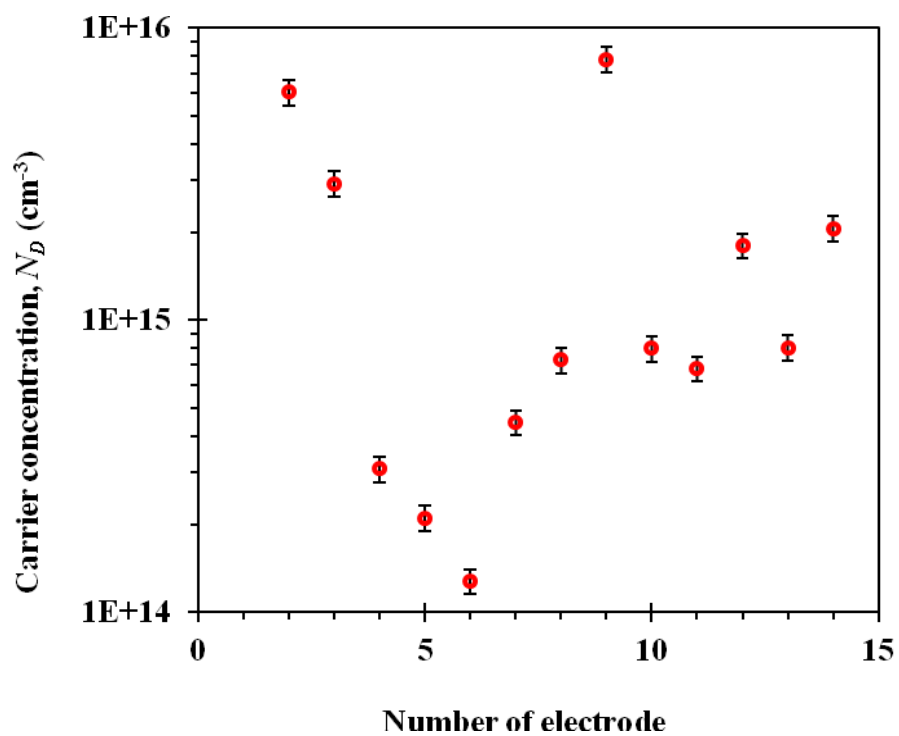


**Figure S5.** Estimated carrier concentration in various nanostructured SnS thin films deposited under equal conditions.

**S7.2. Photoresponse under linear sweep voltammetry of various photo anodes made of SnS thin films**

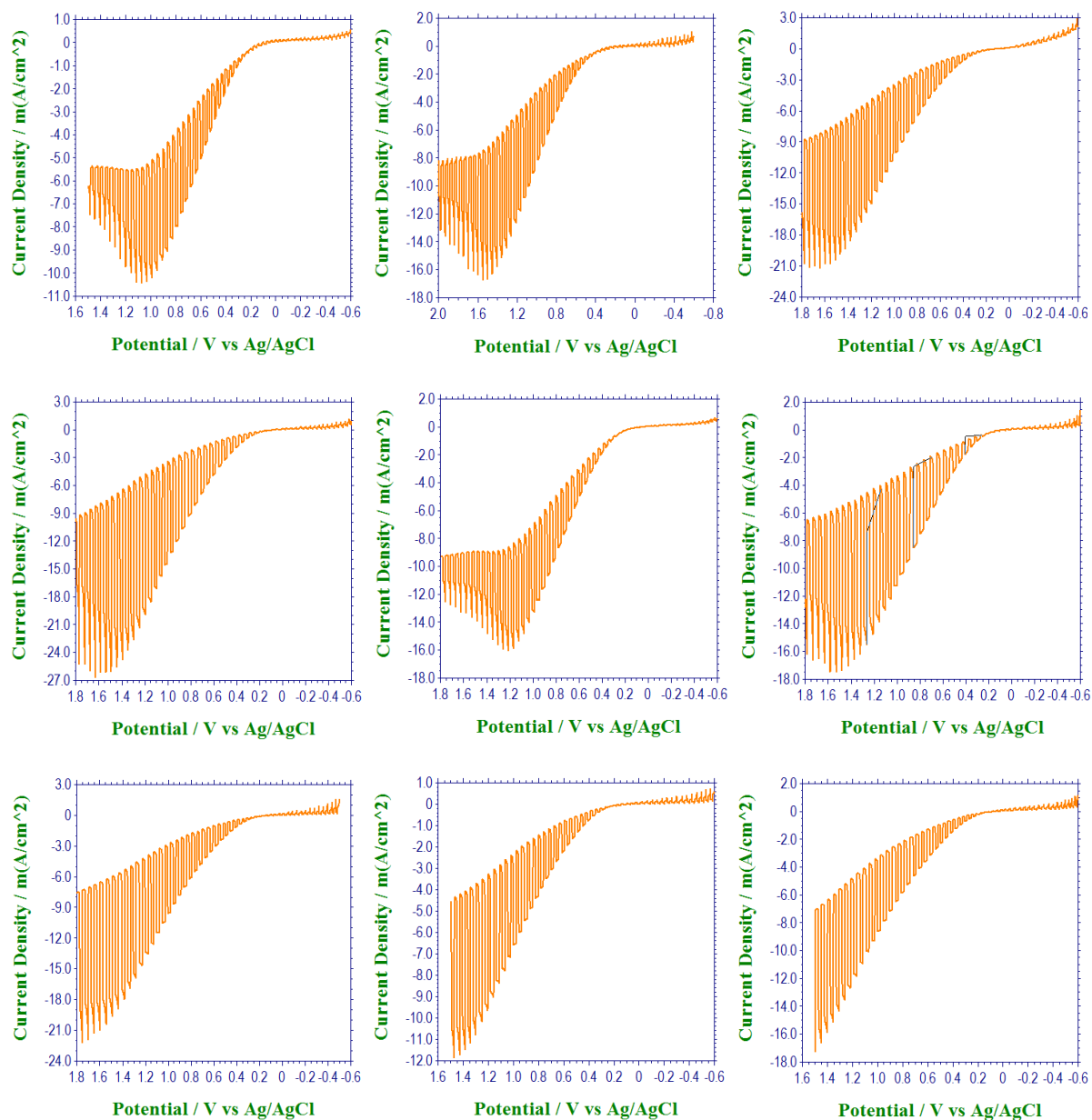


**Figure S6.** The linear sweep photo-voltammogram under pulsed illumination of sprayed SnS-0.1M K<sub>4</sub>Fe(CN)<sub>6</sub> electrolyte interface in the forward and reverse bias regime, where the effect of reproducibility was studied.

## Section S7. Solar-to-chemical conversion Efficiency

The conversion efficiency of PEC cells can be calculated by solar conversion efficiency ( $\eta_c$ ), the ratio of the power used for water splitting to the input light power (Eq. (1)).<sup>[4, 5]</sup>

$$\eta_c = \frac{j_p (E_{rev}^0 - V_{bias})}{I_0} \times 100\%, \quad \text{Equation (1)}$$

where,  $j_p$  is photocurrent density at a certain applied potential,

$E_{rev}^0$  is the standard water splitting reaction potential (1.23 V vs. NHE) at pH = 7,

$I_0$  is the light intensity with unit of W/m<sup>2</sup> (1000 W/m<sup>2</sup> or 100 mW/cm<sup>2</sup>), and

$V_{bias}$  (V vs. RHE) is the applied external potential.

Eq. 1 can reduce to the following equation:

$$\eta_c = \frac{j_p (1.23 \text{ V} - V_{bias})}{I_0}$$

## Section S8. Optical calculations

Model employed for the calculating the total reflectance from the front surface of the electrode immersed in the electrolyte.

### Single layer antireflection coating (ARC) <sup>[6]</sup>;

For the reflectance at normal incidence we define a series of parameters:  $r_1$ ,  $r_2$ , and  $\theta$ . The surrounding region has a refractive index of  $n_0$  (here, electrolyte), the ARC has a refractive index of  $n_1$  (here, SnS front layer) and a thickness of  $t_1$ , and the substrate has a refractive index of  $n_2$  (here, F:SnO<sub>2</sub>).

$$r_1 = \frac{n_0 - n_1}{n_0 + n_1}$$

$$r_2 = \frac{n_1 - n_2}{n_1 + n_2}$$

$$\theta = \frac{2\pi n_1 t_1}{\lambda}$$

For a single layer ARC on a substrate the reflectivity is

$$R = |r^2| = \frac{r_1^2 + r_2^2 + 2r_1 r_2 \cos 2\theta}{1 + r_1^2 r_2^2 + 2r_1 r_2 \cos 2\theta}$$

### Double Layer Anti Reflection Coatings <sup>[7]</sup>

The equations for multiple anti-reflection coatings are more complicated than that for a single layer. First we define a series of parameters:  $r_1$ ,  $r_2$ ,  $r_3$ ,  $\theta_1$  and  $\theta_2$ . The surrounding region has a refractive index of  $n_0$  (Electrolyte), the next layer has a refractive index of  $n_1$  (here, SnS top layer) and a thickness of  $t_1$ , the layer immediately above the FTO has a refractive index of  $n_2$  and a thickness of  $t_2$  and the FTO has a refractive index of  $n_3$ .

$$r_1 = \frac{n_0 - n_1}{n_0 + n_1}$$

$$r_2 = \frac{n_1 - n_2}{n_1 + n_2}$$

$$r_3 = \frac{n_2 - n_3}{n_2 + n_3}$$

$$\theta_1 = \frac{2\pi n_1 t_1}{\lambda}$$

$$\theta_2 = \frac{2\pi n_2 t_2}{\lambda}$$

The reflectivity is then calculated from the above parameters using the following formula:

$$R = |r^2|$$

$$= \frac{r_1^2 + r_2^2 + r_3^2 + r_1^2 r_2^2 r_3^2 + 2r_1 r_2 (1 + r_3^2) \cos 2\theta_1 + 2r_2 r_3 (1 + r_1^2) \cos 2\theta_2 + 2r_1 r_3 \cos 2(\theta_1 + \theta_2) + 2r_1 r_2^2 r_3 \cos 2(\theta_1 - \theta_2)}{1 + r_1^2 r_2^2 + r_1^2 r_3^2 + r_2^2 r_3^2 + 2r_1 r_2 (1 + r_3^2) \cos 2\theta_1 + 2r_2 r_3 (1 + r_1^2) \cos 2\theta_2 + 2r_1 r_3 \cos 2(\theta_1 + \theta_2) + 2r_1 r_2^2 r_3 \cos 2(\theta_1 - \theta_2)}$$

The considered refractive index of the SnO<sub>2</sub> and electrolyte is provided in the Fig. S7(a) and (b), respectively.

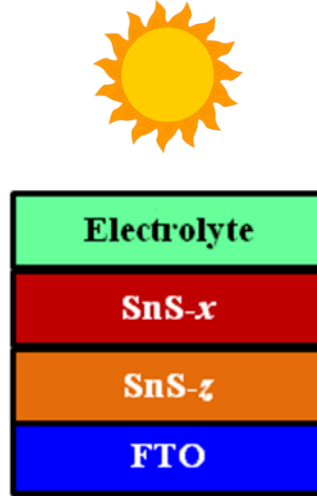


**Figure S7.** Multi layer configuration of layered SnS thin films, where electrolyte is considered as surrounding media.

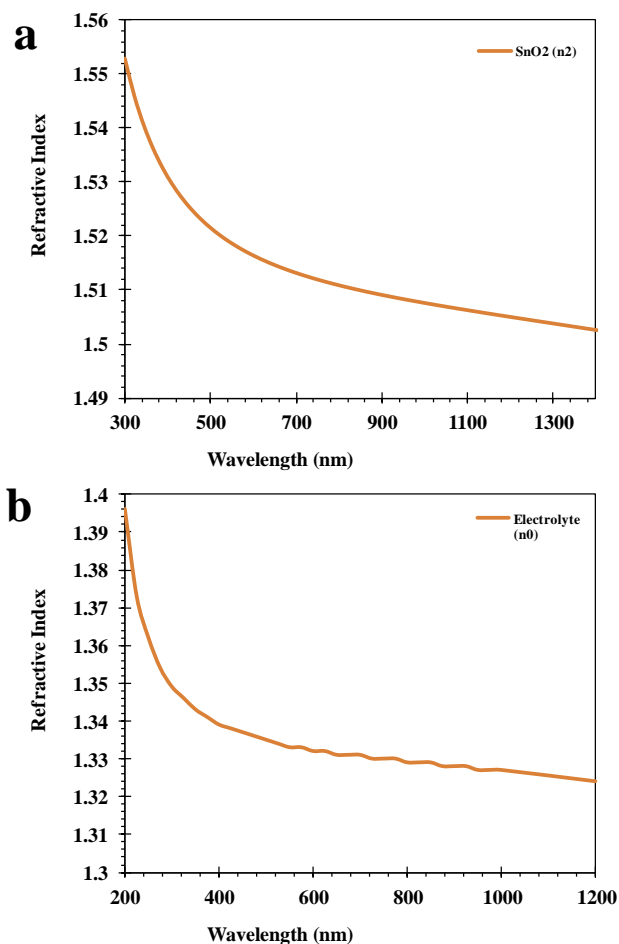


**Figure S8.** Refractive index of (a) SnO<sub>2</sub> and (b) electrolyte [<http://refractiveindex.info/>].

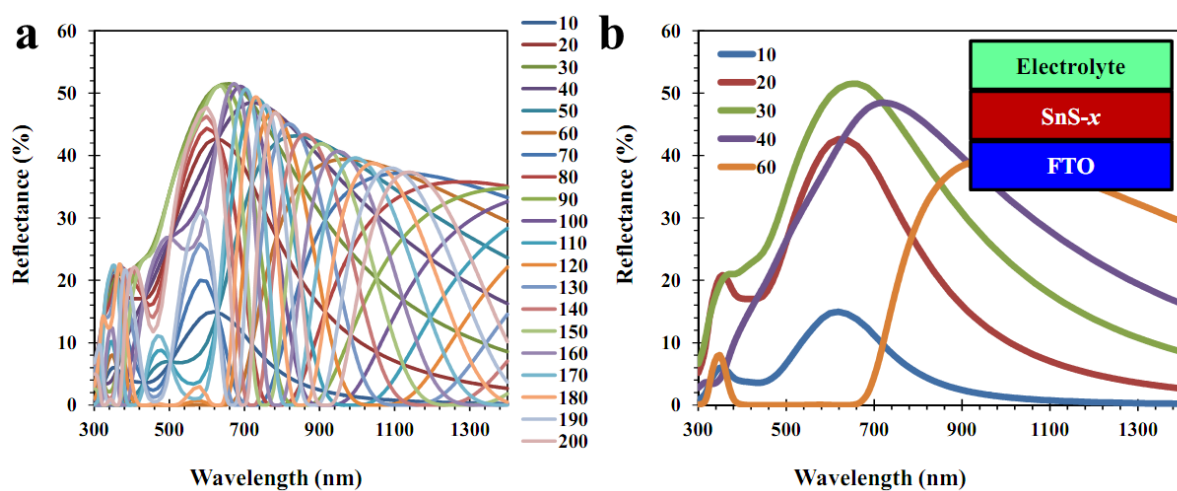


**Figure S9.** Surface reflectance from the SnS surface oriented in *x*-direction over the FTO substrate. (a) thickness of SnS layer was varied from 10-200 nm and (b) selected thickness where 60 nm thin SnS cause the minimum reflectance in the visible region.



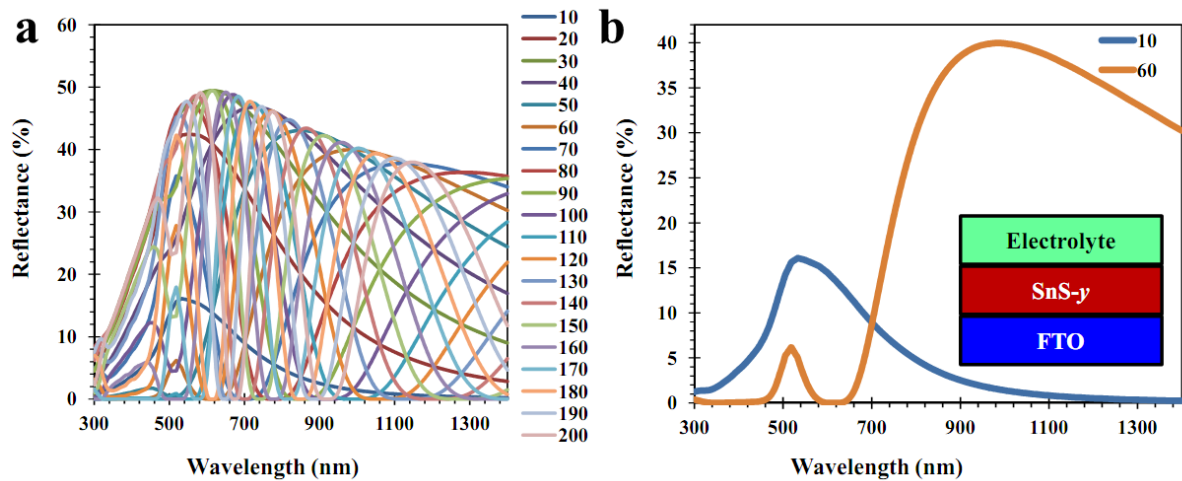


**Figure S10.** Surface reflectance from the SnS surface oriented in y-direction over the FTO substrate. (a) thickness of SnS layer was varied from 10-200 nm and (b) selected thickness.

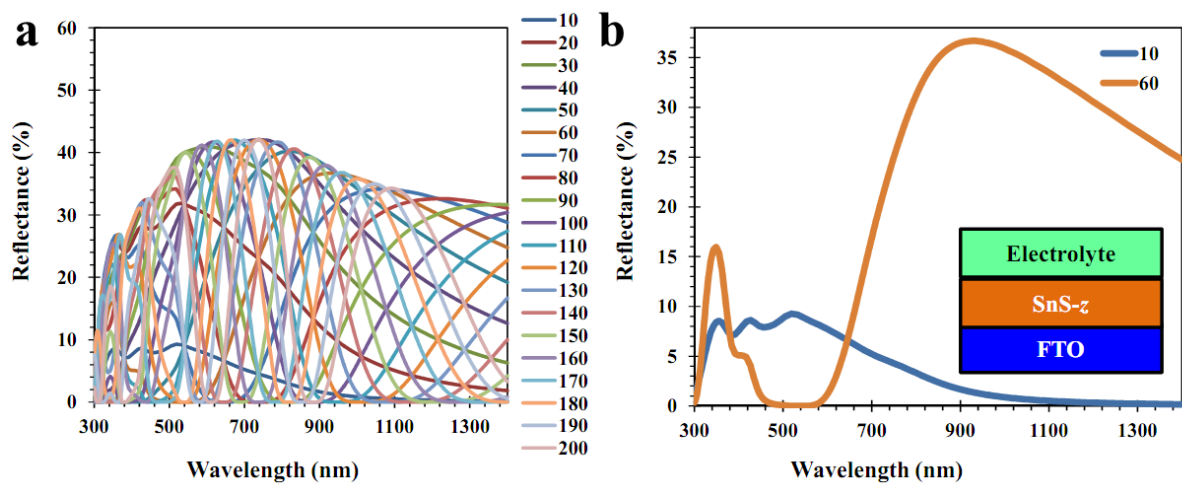


**Figure S11.** Surface reflectance from the SnS surface oriented in z-direction over the FTO substrate. (a) thickness of SnS layer was varied from 10-200 nm and (b) selected thickness.

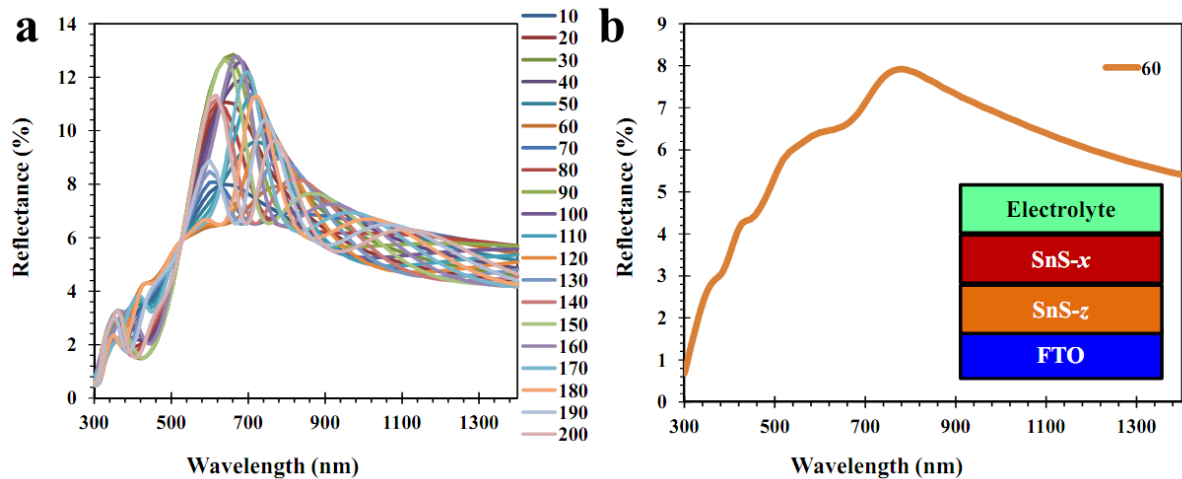


**Figure S12.** Reflectance from the SnS surface oriented in  $x$ -direction over the  $z$ -directional SnS over the FTO substrate. (a) Thickness of SnS layer was varied from 10-200 nm, keeping 10 nm of base SnS layer and (b) selected thickness.

## Section S9. Integrated SnS film PEC cell

A cartoon of the integrated SnS film PEC cell is shown in the following Figure S13 to manifest the configuration that finally obtained the highest photocurrent density ever reported for the SnS film system.

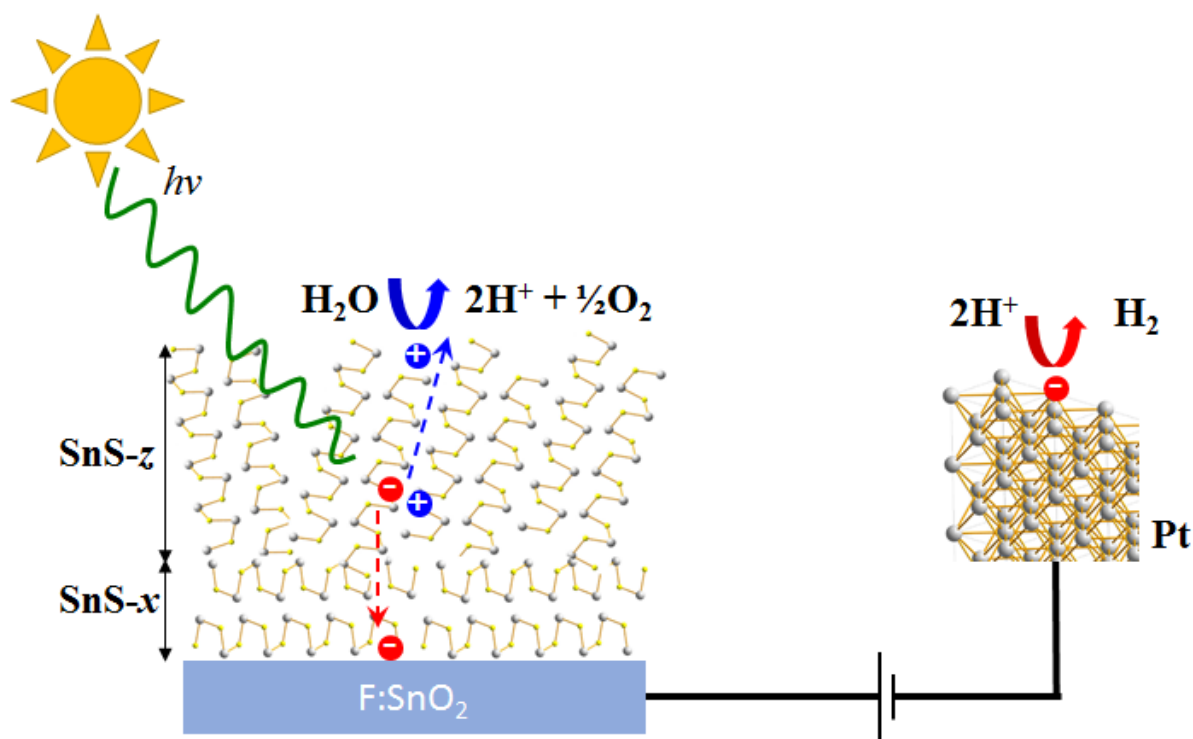


**Figure S13.** Cartoon showing the integrated SnS film with PEC cell.

## Section S10. Stability

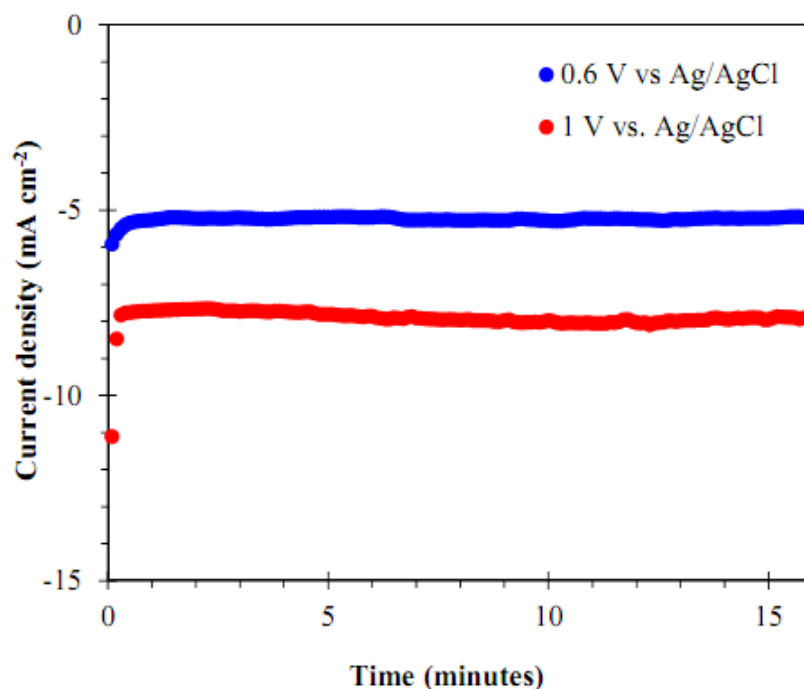


**Figure S14.** Stability study of photoelectrochemical cells with SnS photoanode as working electrode; we have studied the stability for the applied potential of 0.6 V and 1 V vs. Ag/AgCl reference electrode.

The use of such electrolyte ( $\text{K}_4\text{Fe}(\text{CN})_6/\text{K}_4\text{Fe}(\text{CN})_6$ ) has the specific advantage as sacrificial electron scavenging medium over the use of other standard electrolyte such as, 0.5M  $\text{Na}_2\text{SO}_4$ , 0.1M  $\text{Na}_2\text{S}_2\text{O}_3$  or 0.1M KOH. Use of this electrolyte had two advantages in our study: firstly, it stops photo-corrosion of the SnS electrode and secondly, the Mott-Schottky measurement could be performed without a further transfer of the SnS electrode. The onset potential in the case of other electrolyte was more negative than the presented electrolyte, so they were not emphasized in the manuscript. We have studied the stability of water splitting operation at various potential applied to the SnS electrode with reference to Ag/AgCl reference electrode. The observed water splitting phenomena utilizing developed SnS photoanode is shown in Fig.6c. We can see the

evolved gas as hydrogen and oxygen bubbles on the surface of platinum foil (counter electrode) and SnS electrode (working electrode). Fig.S14 shows us the long time operational stability of the photoelectrochemical cell during water splitting operation. Two different potentials 0.6 V and 1 V vs. Ag/AgCl reference electrode were studied. The SnS photoanode offered stable current density characteristics while water splitting operation over the durations of 15 minute.

## Reference

- [1]. Vidal, J.; Lany, S.; d’Avezac, M.; Zunger, A.; Zakutayev, A.; Francis, J.; Tate, J. Band-structure, optical properties, and defect physics of the photovoltaic semiconductor SnS. *Appl. Phys. Lett.* **2012**, *100*, 032104.
- [2]. Nakaoka, K.; Ueyama, J.; Ogura, K. Photoelectrochemical behavior of electrodeposited CuO and Cu<sub>2</sub>O thin films on conducting substrates. *J. Electrochem. Soc.* **2004**, *151*, C661-C665.
- [3]. van de Krol, R.; Grätzel, M. *Photoelectrochemical hydrogen production*. vol. **102** (Springer, 2011)
- [4]. Bak, T.; Nowotny, J.; Rekas, M.; Sorrell, C. C. Photo-electrochemical hydrogen generation from water using solar energy. Materials-related aspects. *Int. J. Hydrogen Energy* **2002**, *27*, 991-1022.
- [5]. Walter, M. G.; Warren, E. L.; McKone, J. R.; Boettcher, S. W.; Mi, Q.; Santori, E. A.; Lewis, N. S. Solar water splitting cells. *Chem. Rev.* **2010**, *110*, 6446-6473.
- [6]. [http://pveducation.org/pvcdrom/design/anti-reflection-coatings#footnote1\\_9c2d7pf](http://pveducation.org/pvcdrom/design/anti-reflection-coatings#footnote1_9c2d7pf)
- [7]. <http://pveducation.org/pvcdrom/design/dlarc>